universität wien

MASTERARBEIT

Titel der Masterarbeit

„NMR studies of the intrinsically disordered protein BASP1“

verfasst von

Andrea Gabriele Flamm, BSc

angestrebter akademischer Grad

Master of Science (MSc)

Wien, 2013

Studienkennzahl lt. Studienblatt:	A 066 834
Studienrichtung lt. Studienblatt:	Masterstudium Molekulare Biologie UG2002
Betreut von:	Univ.-Prof. Dr. Robert Konrat

1. Abstract

The human brain acid soluble protein 1 (BASP1) is a N-terminally myristoylated intrinsically disordered protein found in neuronal phosphatidylinositol 4,5-bisphosphate (PIP2) signaling. The exact physiological function(s) of BASP1 remain unclear but it appears to be involved in growth cone guidance and neurotransmitter release. BASP1 is bound to the exterior of synaptic vesicles or the cytosolic side of the plasma membrane. Nevertheless, one important feature of BASP1 seems to be its cholesterol dependent ability to sequester PIP2 into lipid rafts at the presynaptic membrane or at growth cones of axons.

The aim of this work was to investigate, using nuclear magnetic resonance (NMR) and other biophysical methods, the influence of N-myristoylation on the structural dynamics of BASP1, especially the influence this modification could have on its interaction properties. Therefore, we first achieve recombinant expression of BASP1 with and without N-myristoylation. We were able to obtain recombinant N-myristoylated BASP1 by co-expressing human N-myristoyltransferase in *Escherichia coli* cells using a dual expression vector. Additionally, using mass spectrometry, we were able to show that recombinant expression of N-myristoylated BASP1 in minimal medium, necessary for isotope labeling, leads to a mixture of both myristoylated and lauroylated forms.

The structural dynamics of both native and N-myristoylated forms of BASP1 were under investigation. Interestingly, we were able to show that both forms bind Ca^{2+} directly and that Ca^{2+} leads to a detachment of BASP1 from liposomes *in vitro*. This so far unknown feature of BASP1 can prove to be of relevance *in vivo* since BASP1 is involved in processes that are highly calcium dependent, including the PIP2 signaling pathway, neurotransmitter release and growth cone guidance.

2. Table of contents

3. Table of figures

4. Introduction

4.1. BASP1- a neuronal intrinsically disordered protein

The human Brain Acid Soluble Protein (BASP1; also known as NAP-22 and CAP-23) is an intrinsically disordered protein involved in the phosphatidylinositol 4,5-bisphosphate (PIP2) signaling pathway of neurons. It is located at the axonal growth cone and presynaptic membrane [1]. BASP1 colocalizes with PIP2 in lipid rafts, can influence actin dynamics and neurite outgrowth [2] and appears to be involved in neurotransmitter release and synaptic vesicle endocytosis [3]. For an overview of the function of BASP1 see figure 1.

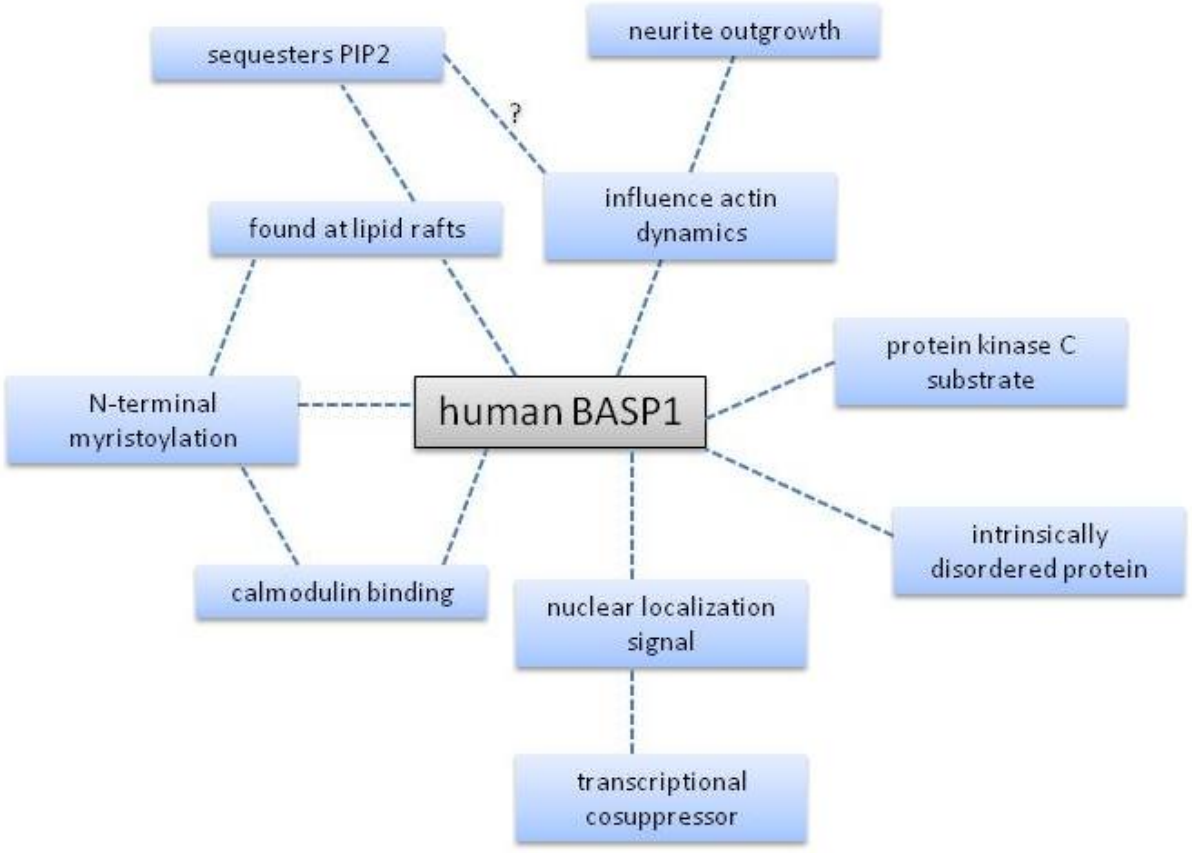

Figure 1: Overview of BASP1s function.

4.2. PIP2 signaling pathway in the neuron

Phosphatidylinositol 4,5-bisphosphate (PIP2) is a key player in cell signaling pathways [4]. It is synthesized from phosphatidylinositol (PI) which is phosphorylated by PI 4-kinase followed by Pl 4-phosphate 5-kinase phosphorylation. PIP2 accounts for only 1% of the cells acidic phospholipids and the corresponding PIP2 phosphatases and kinases are involved in a dynamic cycle of PIP2 modulation. PIP2 is the substrate of phospholipase C; various isoforms of this enzyme are activated by several signaling pathways including G protein coupled receptors and receptor tyrosine kinases. Activated phospholipase C is recruited to the plasma membrane and cleaves PIP2 to produce diacylglycerole (DAG), which stays at the membrane, and soluble inositol 1,4,5-trisphosphate (IP3). Intracellular calcium stores possess IP3-gated Ca^{2+}-channels that open upon IP3-binding, resulting in an increase in cytosolic calcium concentration. DAG together with calcium can activate and recruit protein kinase C to the membrane. PIP2 can get phosphorylated by PI 3-kinase forming phosphatidylinositol 3,4,5-triphosphate (PIP3) that can also act as a second messenger. The different phosphoinositides are located at different regions of the cell and are involved in different processes [4, 5].

In the neuron, PIP2 is involved in neurotransmitter release. It is located at the presynaptic membrane in lipid rafts and in synaptic vesicles where it colocalizes with other molecules that are involved in neuronal signaling. When an action potential arrives at the presynaptic terminal, the cytosolic calcium concentration rises due to opening of voltage-gated calcium channels. This triggers the fusion of synaptic vesicles with the plasma membrane and the release of their content, the neurotransmitters, into the synaptic cleft. Neurotransmitters can dock on receptors on the postsynaptic neuron to pass on the signal. PIP2 is involved in endocytosis, which is the retrieval of synaptic vesicles in order to avoid the consequent fusion of synaptic vesicles with the presynaptic membrane [6]. Besides its function in endocytosis, PIP2 can bind to several ion channels and can regulate their function, including different calcium channels. Another important feature of PIP2 is its influence on actin cytoskeleton dynamics and organization. Other signaling pathways, including Rho family small GTPases, are

“cross-talking” with PIP2 pathways and many actin-binding protein or proteins involved in actin regulation have phosphoinositide binding domains and can directly bind PIP2. They are found in the microdomains where PIP2 and other signaling molecules are clustering [7, 8]. Actin is involved in endocytosis and directed axonal outgrowth during growth cone guidance; both processes are also PIP2 dependent. During neuronal development, growth cone guidance significantly depends on calcium, PIP2- signaling and actin cytoskeleton dynamics. Cytosolic calcium concentration regulates growth cone collapse and localized calcium gradients control repulsion and attraction of axonal outgrowth. Both calcium channels on the plasma membrane and calcium channels on intracellular stores, for example IP3- gated ion channels on the ER, create asymmetric calcium gradients that are necessary for guiding the tip of the axon [9]. For axonal outgrowth, plasma membrane expansion by exocytosis is required and growth cone repulsion includes endocytosis [10].

4.3. Function and location of BASP1 in the cell

BASP1 is present on the external surface of synaptic vesicles [11], in the growth cone of axons [1] as well as in pre- and post-synaptic membranes [12, 13]. In order to be able to bind to membranes, BASP1 is co-translational myristoylated by N-myristoyltransferase; this enzyme catalyzes the covalent attachment of myristic acid, a saturated C14:0 fatty acid, *via* an amide bond on a N-terminal glycine. Once myristoylated, BASP1 colocalizes with PIP2 in a cholesterol dependent manner [2]. BASP1 contains a cholesterol recognition/interaction amino acid consensus pattern (CRAC, [14]). A CRAC is usually composed of L/V-X(1-5)-Y-X(1-5)-R/K and in the case of BASP1 it is located at the N-terminus. BASP1 can bind PIP2 *via* electrostatic interaction with the basic patch on the N-terminus, which was shown by quenching the fluorescence of BODIPYÂ®-TMR–Phosphatidylinositol(4,5)P2 and Phosphatidylinositol(3,4,5)P3 by addition of a N-terminal peptide of BASP1. Only weak quenching was observed for BODIPYÂ®-TMR– Phosphatidylinositol (3,5)P2. Addition of salt reduces the quenching and cleavage by PLC-y abolishes quenching [15]. Mutation of the sole aromatic amino acid Tyr12 abolish the cholesterol-dependent sequestering of PIP2, but not the binding to PIP2 [16]. *In vitro* studies with liposomes show that the activity of phospholipase Cβ,

which cleaves PIP2 and is located in lipid rafts, is reduced in a dose-dependent manner upon addition of BASP1 to the liposomes [17] and there is an inhibition of synaptojanin activity [3], a PIP2 phosphatase involved in clathrin dependent endocytosis [18].

It is not clear what triggers the release of BASP1 from the membrane, but once the protein is not located in the membrane anymore, Ca^{2+}-calmodulin (CaM) binds BASP1 by insertion of the myristoyl moiety into a hydrophobic pocket of CaM and the interaction of several basic amino acids on the N-terminus of BASP1 [19]. Besides CaM binding, BASP1 is a substrate of Protein Kinase C (PKC), with Ser6 being phosphorylated. This post-translational modification abolishes the interaction with calmodulin and the binding of CaM (with a dissociation constant in the low nm range) inhibits the phosphorylation of BASP1 by PKC [20]. These interactions are summarized in figure 2.

Knockout mice lacking BASP1 showed high postnatal lethality and abnormalities in neuronal structures [21]. Overexpression of BASP1 in neurons stimulates neurite outgrowth. Expression of the mutant Ser6Ala that abolishes PKC phosphorylation produced a comparable phenotype whereas mutation of Gly2Ala, which impairs myristoylation, led to no observable neurite outgrowth [22]. These experiments clearly indicate an important role of BASP1 in neuronal development and the substantial impact of co- and post-translational modification in these processes.

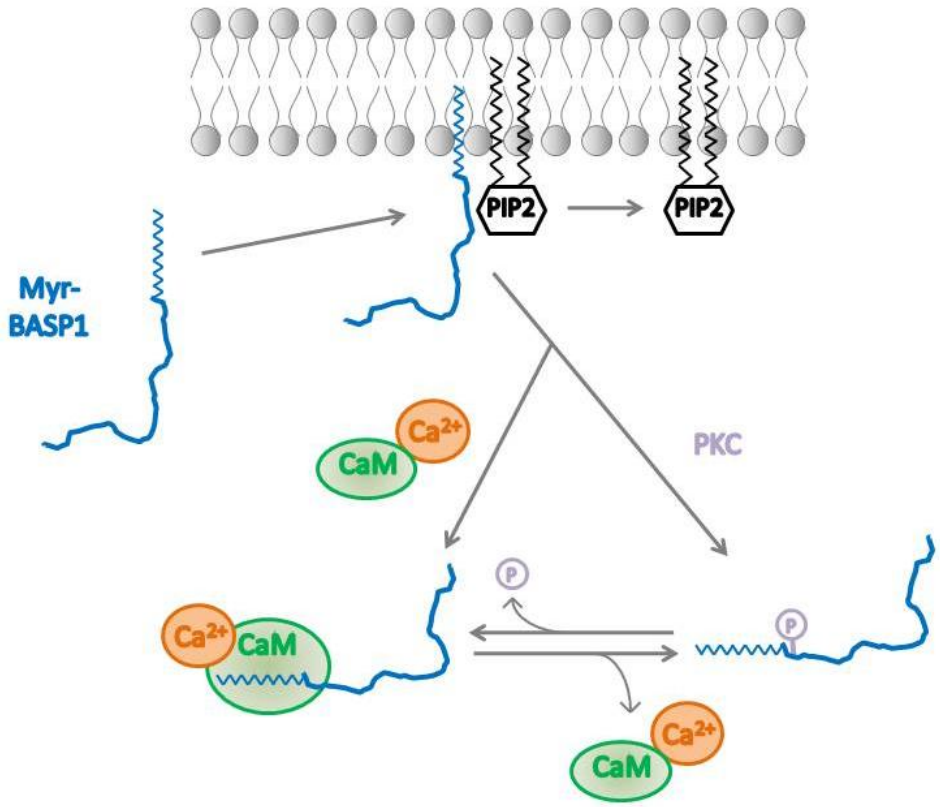

Figure 2: Model of the interaction of BASP1 in lipid rafts. Myristoylated BASP1 is binding to the cytosolic side of the plasma membrane and sequesters PIP2 in a cholesterol- dependent manner. Once the protein is detached from the membrane, it can either get phosphorylated on Ser6 by Protein Kinase C (PKC) or interact with Ca^{2+}-calmodulin (CaM). Once PIP2 is released, it can act as a signaling molecule or can get modified.

4.4. BASP1 in the nucleus

Additionally to its physiological function in neurons, BASP1 is also found in the nucleus. BASP1 has a nuclear localization signal (residues 6-25) and it can be sumoylated by SUMO-3 at Lys79 and Lys84, possibly leading to a relocalization into nuclear bodies [23]. Besides being present in neuronal tissues, BASP1 is abundant in the central nervous system, but it is also present in lungs, thymus, heart, kidney, testis and liver in mouse embryo [24, 25]. It is found in the cytoplasm and nucleus of developing nephron structures and in highly specialized cells in the adult kidney (podocyte cells) where it partially colocalizes with WT1, a transcriptional regulator and tumor suppressor that requires BASP1 as a transcriptional cosuppressor [24]. WT1 and BASP1 occupy several promoters, including *c-myc*. [23].

Transformation of chicken embryo fibroblasts with *v-myc* leads to a down regulation of BASP1 on both the mRNA and protein level. The BASP1 gene contains a myc-responsive regulatory region. Co-expression of myc and BASP1 inhibited cell-transformation as well as myc targeted gene expression [26].

4.5. Physico-chemical parameters of human BASP1

Both the CD spectra of BASP1 [27] and the reported heat-stability [1] support the assumption that BASP1 is an intrinsically disordered protein (IDP). Characteristics of BASP1 include an acidic pI of 4.6 and an anomalous behavior on SDS-PAGE, showing an apparent molecular weight of about 50kDa, whereas the calculated molecular weight is only 22.7kDa. The protein has 227 amino acids (see figure 3) with the most abundant amino acids being alanine (25.1%), glutamate (18.9%), lysine (14.1%) and proline (12.3%). The fact that several amino acids are completely missing, including arginine, cystein, histidine, isoleucine, methionine, phenylalanine and tryptophane and that there is only one aromatic amino acid, namely Tyr12, makes the protein highly hydrophilic. The N-terminal domain is composed of a basic patch and includes a nuclear localization signal and the Protein Kinase C (PKC) phosphorylation site on Ser6.

```
      *  10         20         30         40         50         60
MGGKLSKKKK GYNVNDEKAK EKDKKAEGAA TEEEGTPKES EPQAAAEPAE AKEGKEKPDQ

        70         80         90        100        110        120
DAEGKAEEKE GEKDAAAAKE EAPKAEPEKT EGAAEAKAEP PKAPEQEQAA PGPAAGGEAP

       130        140        150        160        170        180
KAAEAAAAPA ESAAPAAGEE PSKEEGEPKK TEAPAAPAAQ ETKSDGAPAS DSKPGSSEAA

       190        200        210        220
PSSKETPAAT EAPSSTPKAQ GPAASAEEPK PVEAPAANSD QTVTVKE
```

Figure 3: Primary sequence of human BASP1. The PKC phosphorylation site is marked with an asterisk on Ser6. The N-terminal methionine is cleaved off and a myristoyl moiety is added at Gly2.

4.6. Intrinsically disordered proteins

Many proteins are fully or partly unfolded under native conditions [28]. These proteins lack a stable tertiary fold and are called intrinsically disordered proteins (IDPs). Protein disorder seems to increase with complexity of cellular systems, which is reflected by the fact that among eukaryotic proteins, IDPs are more common than in prokaryotes [29] and that they are abundant in regulatory and signaling pathways. IDPs often undergo post-translational modifications such as acylation, phosphorylation or ubiquitination and due to the flexible nature of those proteins, these modifications are expected to have a substantial impact on their structural dynamics and ligand binding properties. Their heterogeneous conformational space enables IDPs to interact with many different binding partners. IDP can undergo folding-upon-binding, meaning that in the native state, the protein is disordered but once a binding partner is interacting with the IDP, it adopts a defined secondary or even tertiary structure. Their inherent structural flexibility is the reason why X-Ray crystallography cannot access IDPs. Folded protein can have one populated energetically low ground state that can lead to crystal formation while the energy landscape of an IDP consists of several local energy minima and the conformations are in a dynamic exchange so that IDPs under native conditions are not capable to produce a suitable crystal. NMR emerged as the major tool for investigation on IDPs as it offers unique opportunities for structural and dynamic studies of IDPs with atomic resolution. NMR can provide information about an IDPs local transient secondary structure with atomic resolution based on chemical shift measurements and scalar couplings or about long-range transient contacts using paramagnetic relaxation enhancement. Chemical shifts report on the backbone conformational preference of the individual residues in a protein because local environment of a nucleus is sensitive to primary, secondary and tertiary structure. By comparing random coil chemical shifts with the measured chemical shift, conclusions about the local structural preferences are possible [30]. Structure elements like an alpha helix results in a change in dihedral angles and this leads to a deviation from random coil chemical shift. For example the $^{13}C\alpha$ and $^{13}C'$ chemical shift increases when the residue is found in an alpha helix and decreased when found in a beta sheet [31].

As expected for an IDP, the ^{1}H-^{15}N- HMQC of BASP1 shows a narrow peak dispersion compared to a folded protein (see figure 5a and 5b). Secondary chemical shifts ($^{13}C'$, $^{13}C\alpha$, $^{1}H\alpha$) resemble random coil structure (see figure 4), with most of the protein being in extended conformation (positive $^{1}H\alpha$ chemical shift differences) except for the N-terminal part that seems to have a higher helical propensity [32].

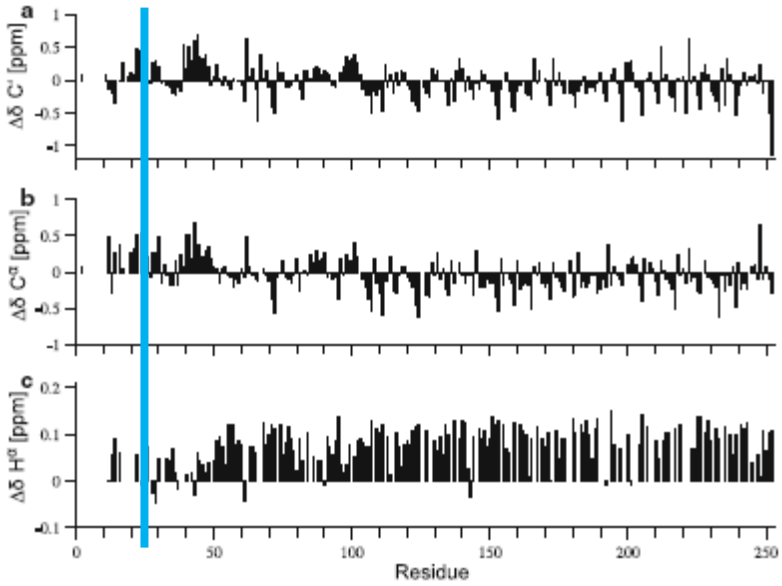

Figure 4: Chemical shifts (a) $^{13}C'$, (b) $^{13}C\alpha$ and (c) $^{1}H\alpha$ of human BASP1 (reprinted from Geist et al [32]). Here the primary sequence numbering is based on human BASP1 with a N-terminal tag and the protein starts at residue 27 (indicated by the blue bar).

Figure 5: (a) sofast ^{1}H-^{15}N-HMQC spectrum of the intrinsically disordered protein human BASP1. Complete signal assignment is available in the BioMagResBank http://www.bmrb.wisc.edu with the BMRB accession number 18417.

(b) ^{1}H-^{15}N- HSQC of Ca^{2+}/calmodulin in 20mM Bis-Tris buffer pH=6.0 with 50mM NaCl and 2mM calcium. Note the difference of the dispersion in the proton dimension between the IDP BASP1 (a) and the folded protein Ca^{2+}-calmodulin (b).

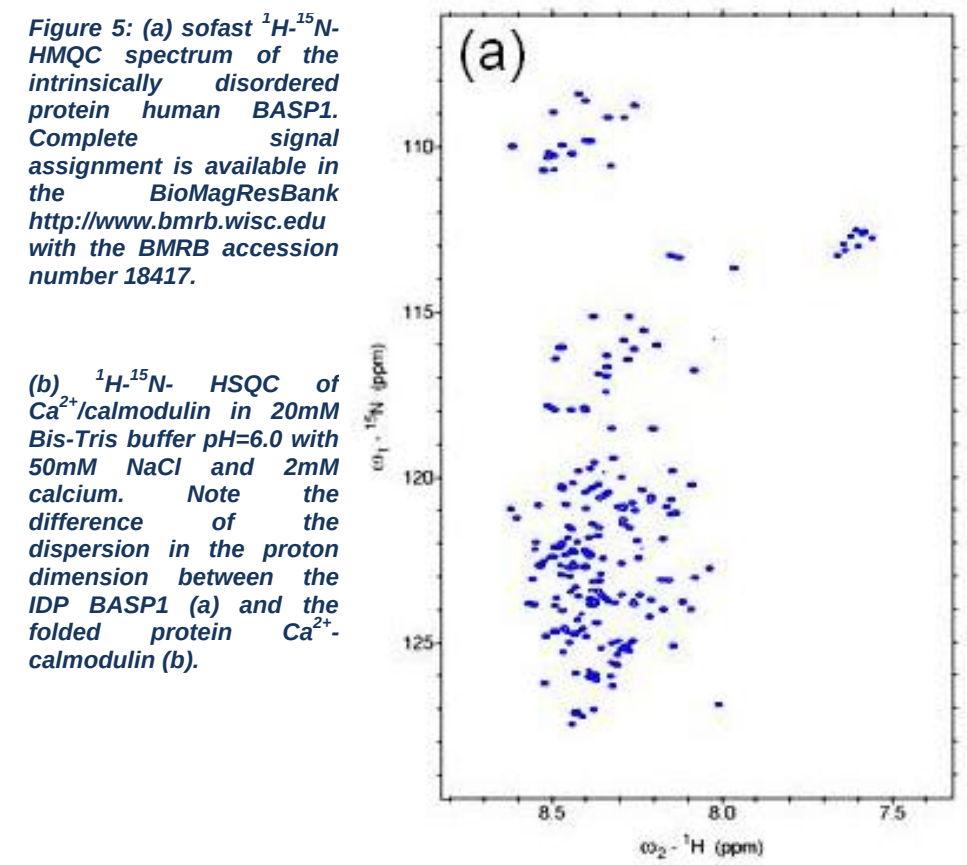

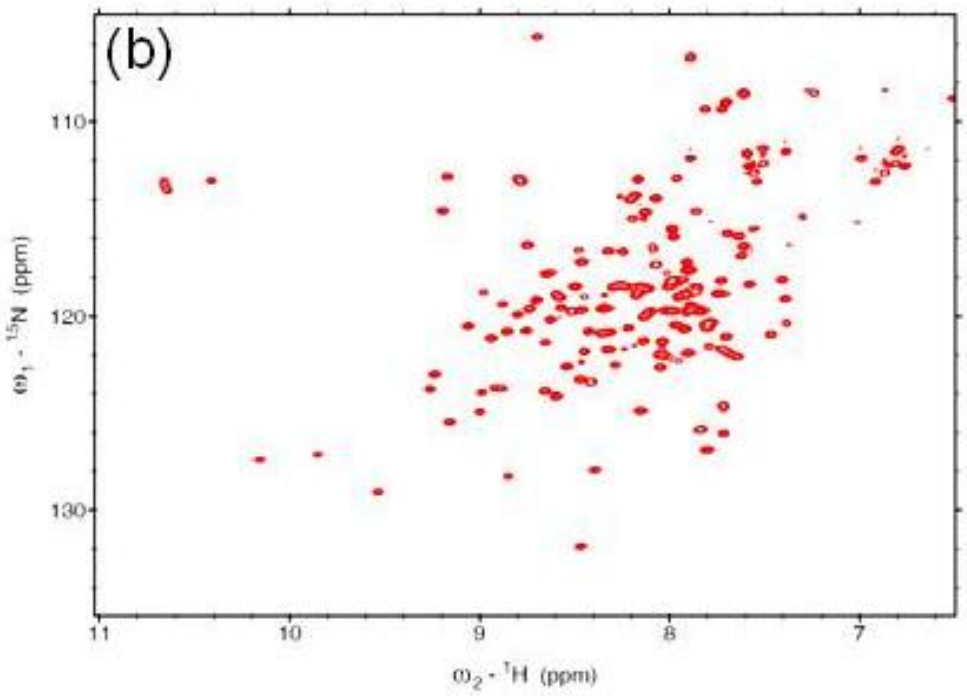

4.7. Purpose of this work

The purpose of this work is to study, mainly by NMR, BASP1s structural dynamics. Since the protein is involved in the neuronal PIP2- signaling pathway, the influence of N-myristoylation on the interaction with calcium/calmodulin and brain derived liposomes will be the main focus of this study. The exact function(s) of BASP1 in the cell still remains unclear, but the results presented in this work could shed some light on the surprising abilities of this intrinsically disordered protein and its potential role(s) in neuronal signaling pathways.

Performed experiments include

- Liposome binding assay of myristoylated and unmyristoylated BASP1 with Ca^{2+} and CaM
- NMR studies of BASP1 including binding to calcium and liposomes
- Expression of ^{15}N-labeled myristoylated BASP1

5. Material

Bis-Tris buffer NMR measurement buffer	20mM Bis-Tris 50mM NaCl → pH= 6.0 →ad 1L H_2O
CaM resuspension buffer	PBS 0.5mM EDTA cOmplete Mini protease inhibitor (Roche)
CaM cleavage buffer	TBS 1mM DTT 5mM EDTA
CaM storage buffer	Bis-Tris buffer 1mM EDTA
LB Broth (Lennox) rich media	20g for 1L of H_2O →autoclave at 121°C
10 x M9	67.8g Na_2HPO_4 x 2 H_2O 30g KH_2PO_4 5g NaCl →pH= 7.4 →ad 1L H_2O
M9 minimal mediafor ^{15}N- labeling of proteins	100mL 10x M9 1g $^{15}NH_4Cl$ →ad 1L H_2O →autoclave at 121°C add 10mL 100x trace element solution 100µL 1M $CaCl_2$ 2mL 1M $MgSO_4$ 20mL 20% glucose solution 1mM antibiotic

Myristic acid solubilization process	5mM myristic acid solution in H_2O →incubate in water bath at 54°C and adjust the pH to 9.0 with NaOH until everything is dissolved
10x PBS	80g NaCl 2g KCl 14.4g Na_2HPO_4 x 2 H_2O 2.4g KH_2PO_4 →pH= 7.4 →ad 1L H_2O
PBS	100mL 10x PBS →ad 1L H_2O
HS PBS High salt PBS	100mL 10x PBS 1.5M NaCl 20mM imidazole →ad 1L H_2O
HI PBS High imidazole PBS	100mL 10x PBS 500mM imidazole →ad 1L H_2O
SDS PAGE destaining solution	30% EtOH 10% HOAc 60% H_2O
SDS PAGE running buffer	2g SDS 6g TrisHCl 28.68g glycine ad 2L H_2O
2x SDS PAGE sample buffer	120mM TrisHCl pH=6.8 6% SDS 20% glycerin 0.01% bromphenol blue 10% β-mercaptoethanol

SDS PAGE separating gel	0.67mL TrisHCl pH=9.0 2mL 40% PAA (37.5:1) 2.67 mL H2O 26.67µL 20% SDS 3.85µL TEMED 16.67µL APS
SDS PAGE stacking gel	0.29mL Tris HCl pH=6.8 0.29mL 40% PAA (19:1) 1.75 mL H_2O 5.83µL 20% SDS 3.85µL TEMED 11.67µL APS
SDS PAGE staining solution	5g Serva Blue G-250 500mL MeOH 100mL HOAc 400mL H_2O
10x TBS	500mM Tris 1.5M NaCl →pH= 7.5
TBS	100mL 10x TBS →ad 1L H_2O
10x Thrombin cleavage buffer	500mM TrisHCl 1.5M NaCl 25mM $CaCl_2$ →pH= 8.0 →ad 1L H_2O
Thrombin cleavage buffer	100mL 10x Thrombin cleavage buffer 1mM β-mercaptoethanol 20mM imidazole →ad 1L H_2O

100x Trace element solution	5g/L EDTA
	0.83g/L $FeCl_3$ x 2 H_2O
	0.084 g/L $ZnCl_2$
	0.013 g/L $CuCl_2$ x 2 H_2O
	0.010 g/L $CoCl_2$ x 2 H_2O
	0.010 g/L H_3BO_3
	0.0016 g/L $MnCl_2$ x 4 H_2O

6. Methods

6.1. Recombinant myristoylation in minimal media for the expression of a ^{15}N-labeled sample

Expression of myristoylated BASP1 is done by using the single vector system pETDuet-1 for coexpression of human BASP1 and human N-myristoyltransferase in *Escherichia coli* cells [33]. BASP1 is fused to an uncleavable C-terminal His6-tag. The amino acid sequence of the C-terminal extension is LEHHHHHHH. To check the efficiency of the myristoylation protocol in minimal media, that is required for isotopic labeling of the protein, the samples are checked by mass spectrometry. The ammonium chloride that is used is unlabeled so that the mass of the protein does not need to be recalculated for analysis of a ^{15}N- labeled sample. Expression was done in *E.coli* strain T7 at 37°C using either rich medium LB or minimal medium M9. 10mL of overnight culture in LB are used for 1L of medium. Ten minutes before the induction, myristic acid was added to the growth medium for a final concentration of 50µM. The expression is induced at an A_{600nm} of 0.6-0.8 by adding 0.8mM IPTG. Expression was carried out for either 4h or overnight (~16h) at 30°C. The cell pellet (after centrifugation at 5000 rpm for 15min) was resuspended in 30mL PBS for 1L of culture. Breaking the cells is done by sonication (3 min of 50% amplitude) and the supernatant after centrifugation at 18000 rpm for 20 min was pressed through a 0.45 µm filter before loading it on a Ni^{2+}-loaded HiTrap 5mL affinity column (GE healthcare). After a washing step with HS-PBS, the protein was eluted *via* a linear gradient of HI-PBS using 18 column volumes. The fractions containing the protein were concentrated and the buffer was exchanged to NMR measurement buffer using an Amnicon Ultra-15 centrifugal filter device 10 000 NMWL. The protein concentration was measured by Pierce™ BCA Protein Assay Kit.

6.2. Expression of unmyristoylated BASP1 with a cleavable His6-tag in minimal medium

For the expression of the unmyristoylated form of BASP1 in minimal medium for a ^{15}N labeled sample, the vector pET29b with a His6-tag and a thrombin cleavage site was used. The amino acid sequence that is fused to the C-terminus of the protein is GDLGTLVPR*GSMAISDPNSSSVDKLAAALEHHHHHH with the asterisk marking the site of thrombin cleavage. Expression was done in *E.coli* strain Rosetta(DE3)pLysS. 10mL of an overnight culture in LB is added to the minimal medium M9 at 37°C. The expression is induced at an A_{600} of 0.6-0.8 by adding 0.8mM IPTG. Expression was carried out overnight (~16h) at 30°C. The cell pellet (after centrifugation at 5000 rpm for 15min) was resuspended using 30mL PBS for 1L of culture. Breaking the cells is done by sonication (3 min of 50% amplitude) and the supernatant after centrifugation at 18000 rpm for 20 min was pressed through a 0.45 µm filter before loading it on a Ni^{2+}-loaded HiTrap 5mL affinity column (GE healthcare). After a washing step with HS-PBS, the protein was eluted *via* a linear gradient of HI-PBS using 18 column volumes. The fractions containing the protein were concentrated using an Amnicon Ultra-15 centrifugal filter device 10 000 NMWL to get an end volume of 1mL. The sample was dialyzed at 4°C overnight against 1L of thrombin cleavage buffer with a spatula tip of thrombin added to the sample. The sample was loaded again on the HiTrap with the same procedure described before and a buffer exchange to the NMR measurement buffer with the fractions containing the protein were done using an Amnicon Ultra-15 centrifugal filter device 10 000 NMWL. The protein concentration was measured by Pierce™ BCA Protein Assay Kit.

6.3. Expression of calmodulin

For the expression of unlabeled calmodulin, the vector pETM11 with a cleavable His6-tag and a TEV cleavage site was used. Expression was done in *E.coli* strain T7. 10mL of an overnight culture in LB is added to 1L of LB at 37°C. The expression is induced at an A_{600} of 0.6-0.8 by adding 0.8mM IPTG. Expression was carried out overnight (~16h) at 30°C. The cell pellet (after centrifugation at 5000 rpm for 15min) was resuspended

using 30mL CaM resuspension buffer for 1L of culture. Breaking the cells is done by sonication (3 min of 50% amplitude) and the supernatant after centrifugation at 18000 rpm for 20 min was pressed through a 0.45 µm filter before loading it on a Ni^{2+} -loaded HiTrap 5mL affinity column (GE healthcare). After a washing step with HS-PBS, the protein was eluted using 100% HI-PBS (~1-2 column volumes). The fractions containing the protein were concentrated using an Amnicon Ultra-15 centrifugal filter device 3 000 NMWL to get an end volume of 1mL. The protein was dialyzed against 1L of CaM cleavage buffer. The sample was put on a shaker at 4°C overnight with 1mg TEV for 50mg protein added to the sample. The sample was loaded on the size exclusion column HiLoad16/60using a flow rate of 1mL/min and 150mL of CaM storage buffer. Concentrating the fractions containing the protein were done using an Amnicon Ultra-15 centrifugal filter device 3000 NMWL. The protein concentration was measured by A_{280nm}.

6.4. Folch Liposomes

Liposomes were prepared by drying Folch lipids in chloroform (5mg/ml) under a stream of argon. To make sure no chloroform is left, the lipids are dried in vacuum for 1h in a desiccator. NMR measurement buffer was added for a final concentration of 1mg Folch liposomes per ml and after an incubation time of 30 minutes, the lipids were resuspended and subjected to 3 cycles of freezing (liquid nitrogen) and thawing (hot water) before sonication in a water bath for five minutes. The liposome size was restricted by using an extruder with a 0.4µm filter.

6.5. Liposome binding assay

25µL of liposomes were mixed with 5µg of protein and variable amounts of Ca^{2+}, CaM or EDTA for a final volume of 50µL. The mixture was incubated for 30 minutes and centrifuged at 68,000 rpm for 10min at 22°C using the ultracentrifuge rotor TLA-100.3. 50µL of 2xSDS sample buffer was added to the supernatant and 50µL of buffer and 2xSDS sample buffer were added to the pellet. After incubation of the pellet for 30 min, the samples were analyzed using SDS-PAGE. Relative quantification was done by using ImageJ.

6.6. NMR measurements

The spectra were recorded using a Varian spectrometer operating at 800MHz at 25°C. The final protein concentration is 200µM in Bis Tris Buffer pH 6.0 with 10% D_2O in the sample. Processing and analysis of the spectra was done by using NMRPipe and SPARKY. Using sofast ^{1}H-^{15}N HMQC [34], the chemical shift change $\Delta\delta$ was calculated the following way

$$\Delta\delta = \sqrt{\left(\frac{\Delta\delta_N}{10}\right)^2 + \Delta\delta_H^2}$$

where $\Delta\delta_N$ is the chemical shift change in the nitrogen dimension and $\Delta\delta_H$ is the chemical shift change in the proton dimension. The peak height ratio I/I_0 is calculated by dividing the peak height obtained from the spectrum in the presence (I) of manganese or liposomes by the reference spectrum (I_0).

6.7. Mass spectrometry

The ESI-FT-ICR mass spectrometry was performed by Kathrin Breuker (Institute of Organic Chemistry, University of Innsbruck).

6.8. SDS PAGE

To prepare a 15% gel for SDS PAGE, the SDS PAGE separating gel is poured into the gel caster and isopropanol is added on top. After polymerization, the isopropanol is removed and the SDS PAGE stacking gel is poured on top of the separating gel and the comb is inserted. After polymerization, the gels are stored at 4°C. The samples are mixed with 2xSDS sample buffer and heated up to 95°C prior to the SDS PAGE. Once the samples are added, the gel runs in SDS PAGE running buffer for 50 minutes at 200 volt. The gel is stained in SDS PAGE staining solution for 20 minutes and destained in SDS PAGE destaining solution.

6.9. Pierce™ BCA Protein Assay Kit

Since the extinction coefficient of BASP1 is only 1490 $L.mol^{-1}.cm^{-1}$, measuring the absorption at 280nm does not give a reliable concentration estimation. The Pierce™ BCA Protein Assay Kit (Thermo Scientific) is used to measure the amount of protein. It is based on the biuret reaction, which is the reduction of Cu^{2+} to Cu^{+} by the protein in alkaline surrounding, and the detection of the Cu^{+} ions with a reagent containing bicinchoninic acid. The absorbance is measured at 562nm. With BSA, a standard curve is plotted and the concentration of BASP1 can be calculated based on the absorption and the standard curve (see figure 6).

To measure, 25µL of the sample in various concentrations is added to 500µL of BCA reagent A and 10µL of BCA reagent B. The mixture is incubated at 37°C for 30 minutes and the absorption at 562nm is measured.

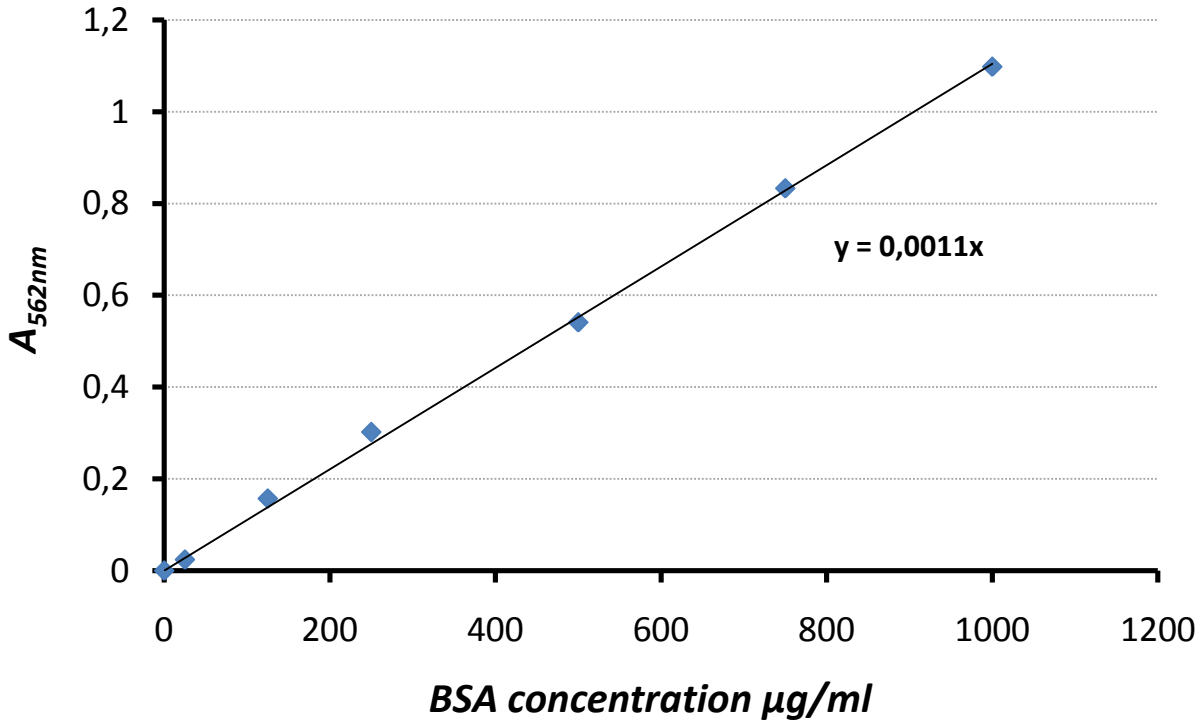

Figure 6: BSA standard curve for the Pierce™ BCA Protein Assay Kit.

6.10. Correlation of the distance of the calcium ion of the co-oordination loop of calmodulin and the paramagnetic effect of manganese on BASP1

Calculations are based on a work by Ubach *et at* [35]. Manganese binding increases the relaxation rate by dipolar interactions that are inversely proportional to the distance between nuclei and Mn^{2+}. Paramagnetic effect of manganese and the distance of the bound calcium to residues of a protein in crystal structures can be combined to get an indication about an unknown binding mode. The distance of the calcium ion in the crystal structure of calmodulin (PDB ID= 1EXR) to the backbone nitrogen of the binding loop residues is measured for all four calmodulin binding loops that are located between residues 20-31, 56-67, 93-104 and 129-140. An average distance $r_{N\text{-}Ca}$to every residue is calculated. The cross peak intensities of sofast^{1}H-^{15}N HMQC spectrum are measured both with and without manganese and both are normalized by the reference without Mn^{2+}. Calculation of ΔI^{-1} is done by taking the difference of the inverted intensities

$$\Delta I^{-1} = I_{Mn}^{-1} - I_{0}^{-1}$$

Where I_{Mn}^{-1} is the inverted normalized intensity of the spectrum recorded with manganese and $I_{0}^{-1}$is the inverted normalized intensity of the reference spectrum. Plotting log(ΔI^{-1}) versus log($r_{N\text{-}Ca}$) should result in a negative slope.

7. Results

7.1. Liposome binding assay of myristoylated and unmyristoylated BASP1

Using Myr-BASP1 and unmyristoylated BASP1, we first focused on the interaction with membranes by a liposome binding assay. Since BASP1 is present in developing neurons, Folch liposomes were used. Folch liposomes contain the major lipids found in the plasma membrane of brain tissues. In general, the lipid composition on the cytosolic side, where BASP1 is located, differs from the lipid composition found on the exterior of the plasma membrane [36]. Lipids that are known to be located on the cytosolic side of synaptic vesicles include cholesterol, phosphatidylcholine, phosphatidylethanolamine, phosphatidylserine and phosphoinositides [37].

As expected, in the absence of calcium and/or calmodulin, the myristoylated form of the protein is completely bound to the liposomes whereas the amount of unmyristoylated protein bound is about 35% (see figure 7). It is interesting to observe that even without N-myristoylation, BASP1 is able to bind to membranes. The control experiment without liposomes excludes the possibility that the amount of protein in the pellet is due to an aggregation of the protein. Surprisingly, at a Ca^{2+}- concentration of 2mM, 50 % of the myristoylated protein is released from the liposome, whereas the unmyristoylated protein is completely released.

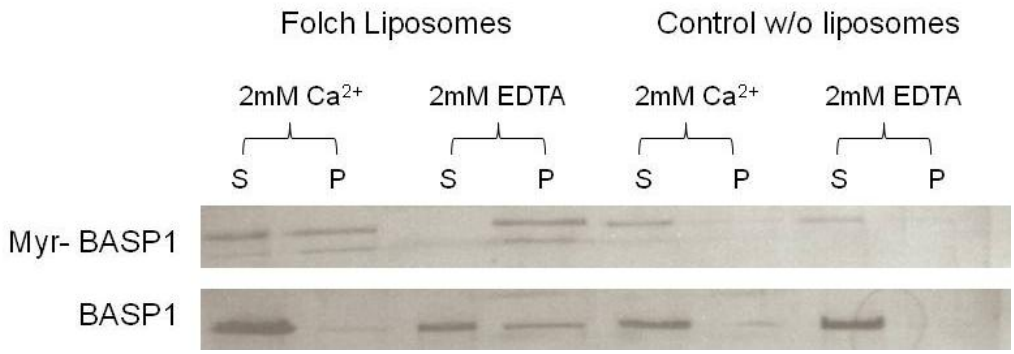

Figure 7: Liposome binding assay. Comparison of the binding abilities of myristoylated (Myr-BASP1) and unmyristoylated BASP1 in the presence and absence of calcium. The relative quantification was done using ImageJ. S: supernatant, P: pellet (liposome bound form)

To look further on this surprising calcium dependent detachment process of Myr-BASP1, we tested the effect of CaM on liposome binding. Upon addition of apo-CaM, no detachment can be observed, which is not surprising because Myr-BASP1 is known to interact only with holo-CaM (see figure 8). Addition of Ca^{2+}-loaded CaM does not trigger membrane detachment (50µM Ca^{2+}). Surprisingly, it seems that calcium on its own is able to trigger the detachment of the protein from the liposomes. Indeed, upon addition of 2mM Ca^{2+}/CaM, there is no change in the ratio of bound/unbound Myr-BASP1 when compared to the addition of 2mM Ca^{2+} alone.

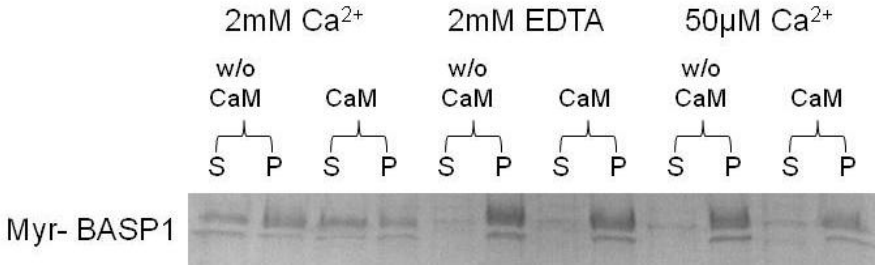

Figure 8: Liposome binding assay with CaM. Comparison of the detachment abilities of Myr-BASP1 in the presence and absence of calcium and/or CaM. The relative quantification was done using ImageJ. S: supernatant, P: pellet (liposome bound form). The CaM concentration is 10µM which is approximately two times equivalent amount to Myr-BASP1.

7.2. NMR studies of BASP1

In order to get more insight, at atomic resolution, on the intriguing calcium binding properties of BASP1, we decided to use solution state NMR to study BASP1 binding properties towards calcium and liposomes. Since our liposome binding experiment showed that even unmyristoylated BASP1 is able to bind to liposomes. We could use isotopically enriched unmyristoylated form of BASP1 for all NMR experiments.

First, in order to determine the binding site of Ca^{2+}, a series of sofast ^{1}H-^{15}N HMQC spectra of unmyristoylated BASP1 were recorded with increasing Ca^{2+} concentrating. By following the chemical shift changes upon addition of Ca^{2+} (see figure 9), we were able to identify one major binding site at residues 59-70. Additionally, there are two possible binding sites with a lower affinity located between residues 130-150, a region which contains several negatively charged residues, and around residues 30-40 (see figure 11a). To further characterize the binding site, the paramagnetic properties of manganese (Mn^{2+}) were exploited. In contrast to the calcium ion, the binding of manganese will result in a decrease of peak height due to increased relaxation rates (see figure 10). The titration with manganese showed an intensity decrease at the same three sites, again with the strongest effect at residues 59-70 (see figure 11b).

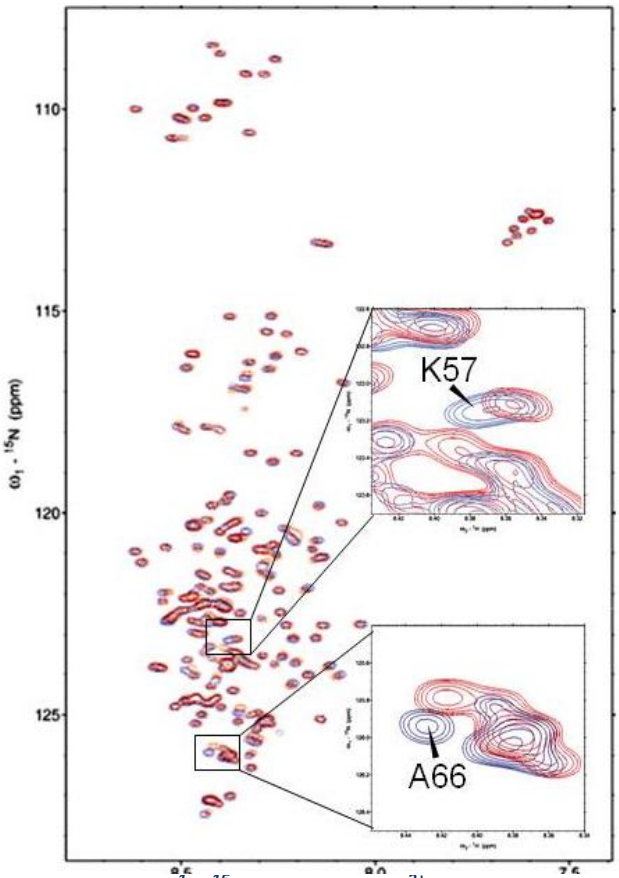

Figure 9: sofast ^{1}H-^{15}N HMQC of Ca^{2+}/BASP1. Titration of BASP1 results in chemical shift change when the reference spectrum (blue) is compared to the spectrum with 10mM calcium (red).

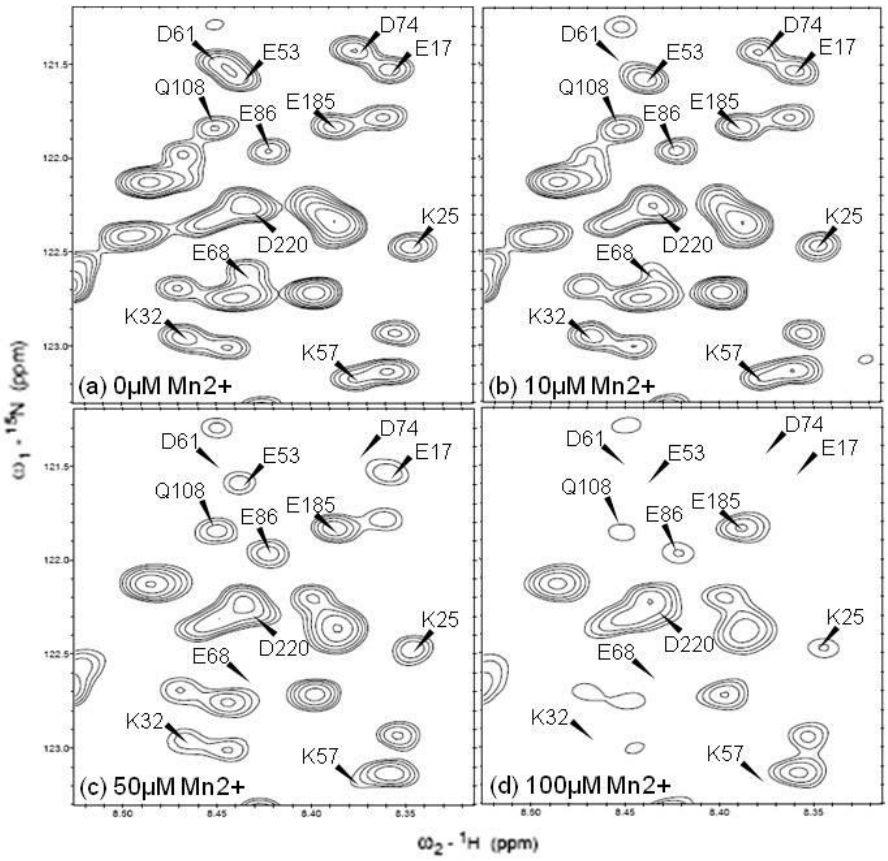

Figure 10: Paramagnetic effect of manganese. Notice that D61 and E68, two residues that are located in the region of large chemical shift changes upon Ca^{2+} binding, show decreased peak height already in the presence of 10µM Mn^{2+} (b).

Next, we studied the binding of BASP1 to liposomes using NMR. Liposomes were added to the unmyristoylated form and the cross peak intensities of the sofast ^{1}H-^{15}N HMQC spectra of the liposome bound form were measured. Local intensity decrease can be observed for BASP1 which indicated a specific binding event. The binding is strongest in the N-terminal part of the protein, up to residue twelve (see figure 12a). This part contains a basic patch and the only aromatic amino acid. It is not clear whether the intensity decrease in the rest of the protein is due to a transient interaction with the liposomes or a change in the relaxation properties of the protein due to the binding of the N-terminal part. In addition, multiple binding modes of the protein would be possible. The intensity of the C-terminal part is unchanged.

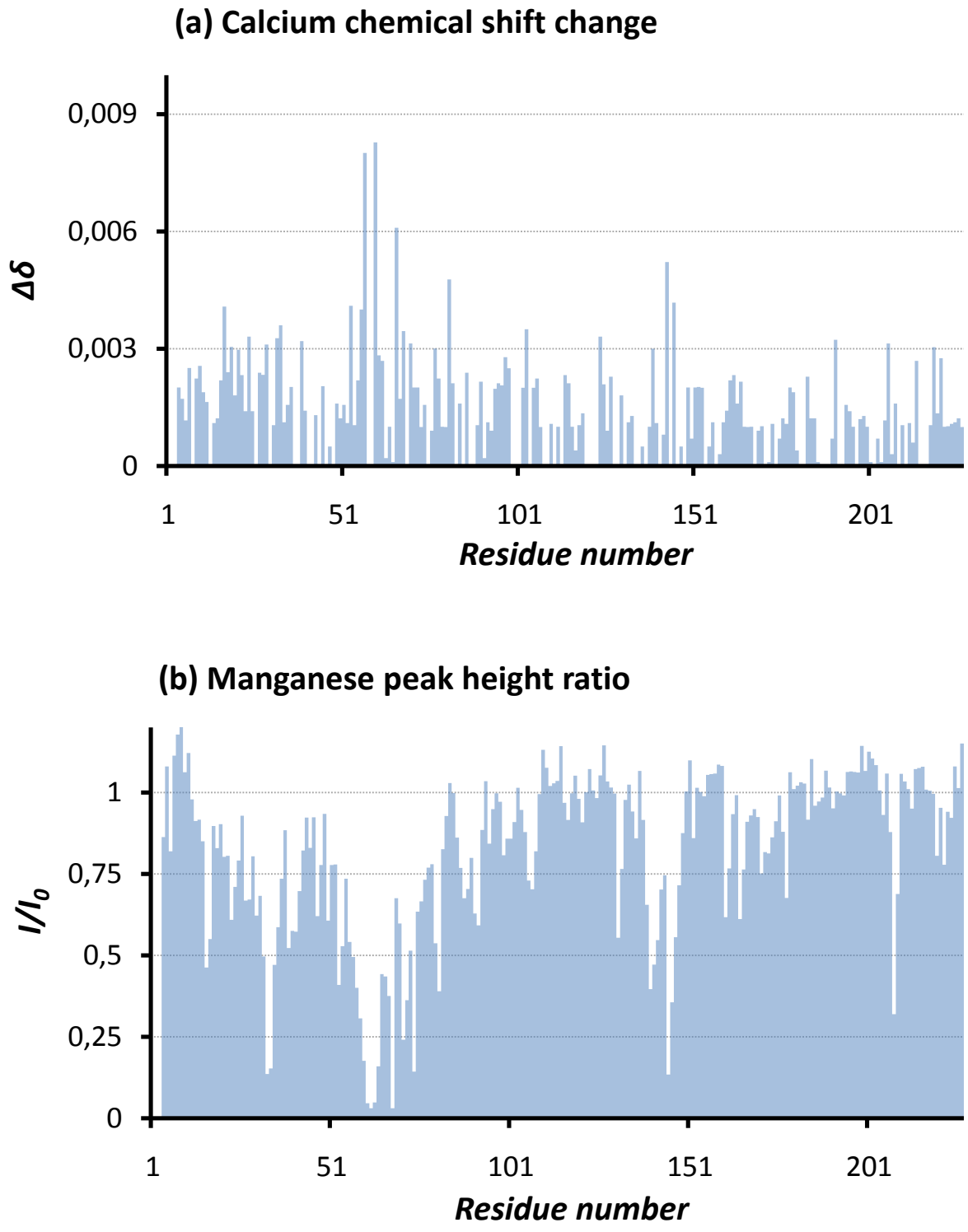

Figure 11: Residue plot of the calcium and manganese titration of unmyristoylated BASP1. The calcium concentration is 2mM and the manganese concentration is 50µM.

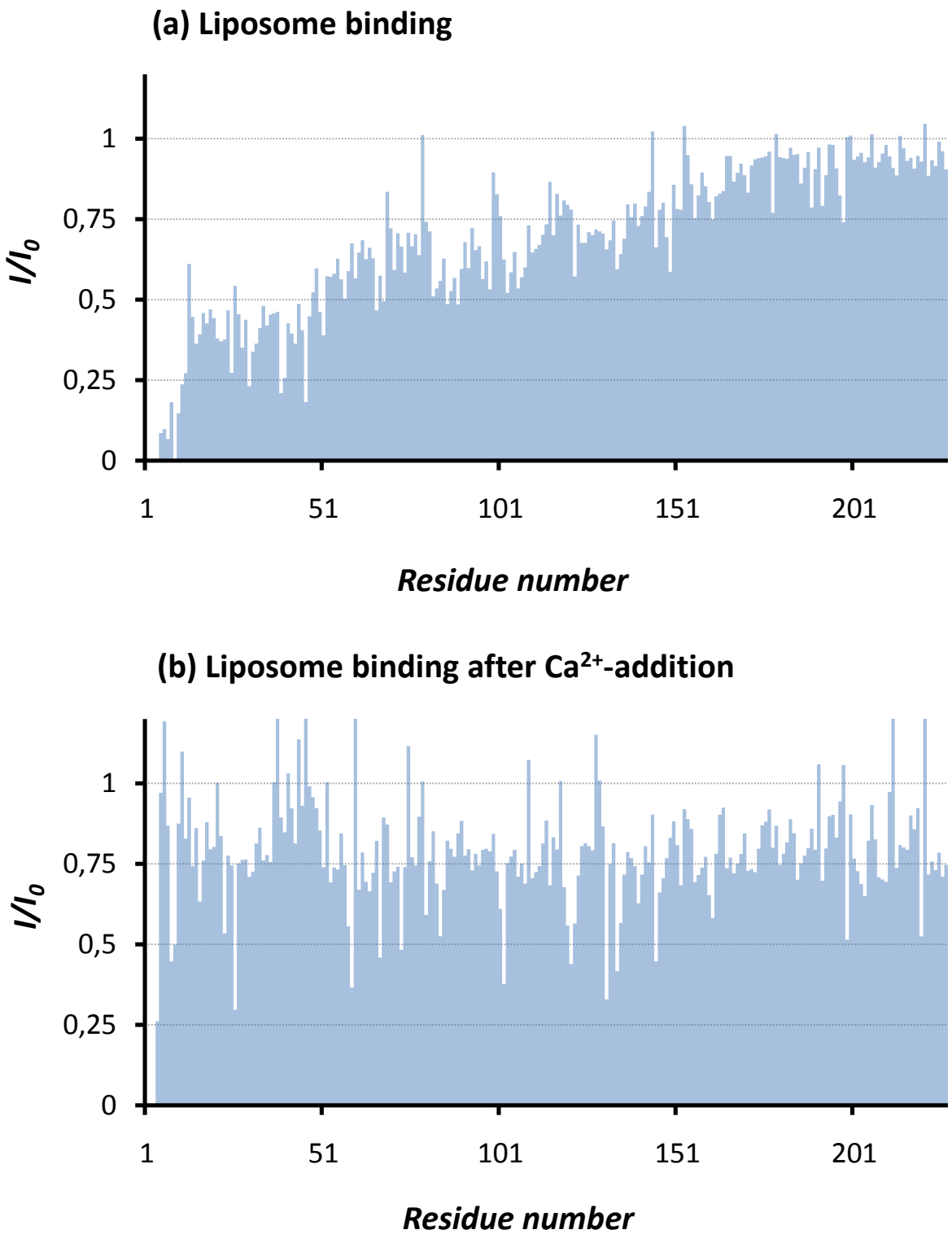

Figure 12: Liposome binding of unmyristoylated BASP1 and the calcium-dependent release. Liposome concentration is 2 mg.mL^{-1}of Folch lipids and the final calcium concentration is 8mM.

In order to confirm the observation that calcium alone can release BASP1 from the membrane, we checked the effect of calcium addition on the liposome bound form of BASP1 (see figure 12b). At 8mM Ca^{2+}, the intensities are restored to about 80% of the reference spectrum (without liposomes). This intensity is the same intensity that is observed after Ca^{2+}- titration without liposomes. This is due to an increase in the ionic strength in the buffer leading to a reduced performance of the coil. Intensities can be restored when tuning, proton pulse and transmitter offset frequency are adjusted.

7.3. Recombinant myristoylation in minimal media for the expression of a ^{15}N-labeled sample

In order to observe the influence of N-myristoylation on BASP1's structural dynamics by NMR, we first had to obtain isotopically labeled protein. This requires the expression of the recombinant protein in minimal medium where the sources of carbon and nitrogen can be selectively isotope-labeled. Recombinant myristoylated protein can be obtained by coexpression of BASP1 (fused to a C-terminal His6-tag) and human N-myristoyltransferase (hNMT) in *Escherichia coli* cells using a single vector system [33] and an external supply of myristic acid. To make sure that this protocol yields to fully myristoylated sample, we first checked the purity of our samples by mass spectrometry (see figure 13). The results show that when BASP1 is expressed in rich medium for 4 hours, the protein is uniformly myristoylated (see figure 13c). When using minimal media, a loss of two CH_2 groups was observed leading to the production of two different acylated forms of BASP1 (see figure 13b and 13d); either with myristic (C14:0) or lauric acid (C12:0). To exclude the possibility that this result is due to impurities of the added myristic acid, it was also checked by mass spectrometry (result not showed here). Only pure myristic acid is added to the growth medium. Therefore, the presence of lauroylated form probably originates from the restricted availability of carbon sources and the enzymatic degradation in minimal medium, which is not the case for LB. The hNMT is known to be not fully substrate specific for myristic acid, but can also attach other saturated and unsaturated acyl-CoAs [38]. The myristoylated form is present to approximately 60% when expressed in minimal medium. The length of the expression does not seem to have an influence on the amount of lauroylated form (4 or 16 hours). On the other hand, expressing the protein in rich medium overnight leads to a slight increase of N-lauroylated form, which confirms that the availability of carbon sources, which starts to decline after long period of growth, is at the origin of the enzymatic digestion of myristic acid (data not shown here). In order to check our hypothesis, we tried to increase the glucose content of the minimal media from 4g/L to 10g/L with the aim to reduce the enzymatic digestion of myristic acid. Unfortunately, increasing the glucose concentration does not change the ratio of myristoylated to lauroylated BASP1

(data not shown here). When the growth medium is supplied with only lauric acid, the sample is entirely lauroylated, which confirm our hypothesis and allow us to obtain a pure lauroylated sample (see figure 13e and 13f).

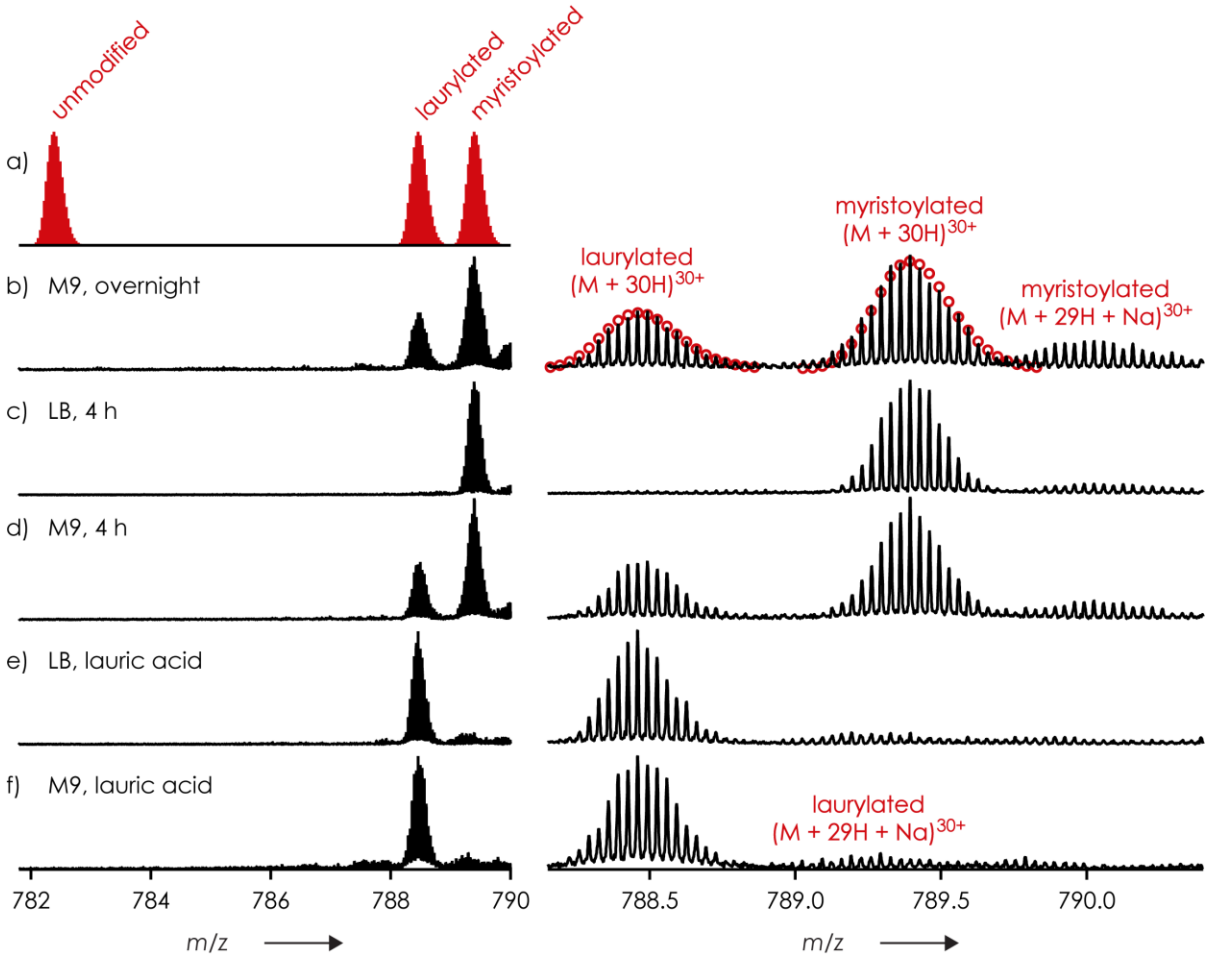

Figure 13: Calculated (a) and measured (b-f) ESI spectra of human BASP1 expressed in E. coli (b) M9, overnight, (c) L4, 4h, (d) M9, 4 h, (e) and (f) LB and M9, respectively, with lauric acid added to the growth medium; red circles in (b) show calculated isotopic profiles for (M + 30H)30+ ions of laurylated and myristoylated protein.

8. Discussion

8.1. Recombinant myristoylation in minimal media for the expression of a isotopically labeled protein

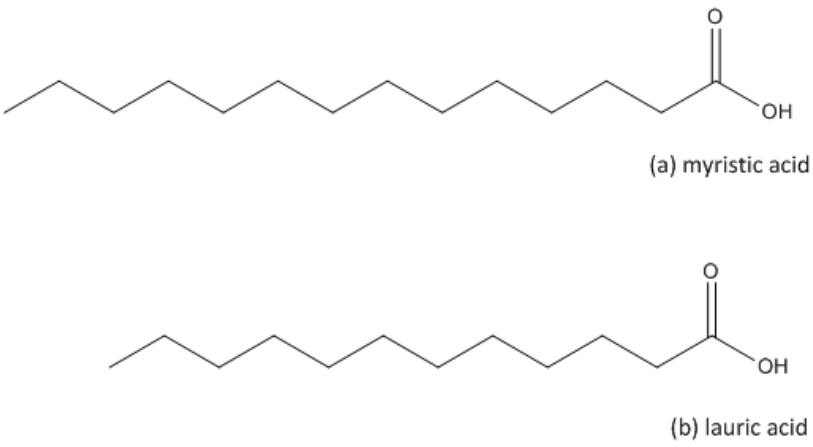

Figure 14: Structure of myristic and lauric acid.

The aim of this work was to study the influence of myristoylation on the structural dynamics of BASP1. Therefore we first had to obtain a ^{15}N labeled uniformly myristoylated sample. The expression had to be done in minimal medium where, beside myristoylation, we observed a second modification that does not occur when expression is performed in rich medium; the attachment of lauric acid to BASP1. Lauric acid is a product of beta-oxidation of myristic acid. *E.coli* can grow on fatty acids as the only carbon source by fatty acid degradation *via* beta-oxidation. Since the minimal medium contains glucose as the sole carbon and energy source, the bacteria starts to use myristic acid, which is added to the growth media, as an additional carbon and energy source whereas in rich media, the bacteria has other carbon and energy sources to use. Expressing overnight in rich medium leads to a slight increase of the modification with lauric acid since the other carbon sources start to get less abundant. The human N-myristoyltransferase is not fully substrate specific for myristic acid and can also attach lauric acid. Indeed, *in vitro* studies of the human N-myristoyltransferase show that the enzyme is able to attach different naturally occurring and synthetic fatty acids [38]. Additionally, lauroylation of proteins that have a myristoylation site on the N-terminus does also occur *in vivo*. Especially in the retina due to its special lipid metabolism [39], several myristoylated proteins are found to be modified with lauric acid (C12:0) and

unsaturated fatty acids (C14:1 and C14:2) [40, 41]. In eukaryotic cells, beta oxidation takes place mainly in the mitochondria but also in peroxisomes resulting in restricted availability of lauroyl-CoAs in the nucleus. But in *E.coli* the availability of both myristic and lauric acid for the N-myristoyltransferase leads to the attachment of both fatty acids at the N-terminus of human BASP. Consequently, the protocol used for the recombinant myristoylation in *E.coli* is not suitable to obtain a homogenous sample when using minimal medium. Our preliminary data show that both forms can be separated by RP-HPLC (data not shown) but, so far, not on a quantitative scale.

Other proteins that are at least partially disordered are also myristoylated, for example HIV-Nef [42] or MARCKS [43]. The influence of the myristoylation on the structural and dynamic features can be addressed by NMR but for that purpose a uniformly modified protein has to be obtained. When expressing myristoylated proteins, isotopically labeled or unlabeled, in other media than rich medium LB using the recombinant *in vivo* myristoylation, one should keep in mind the possibility of other modifications since the human NMT is not fully substrate specific for myristic acid.

Besides the surprising result, that in minimal media, the protein is not homogenously modified with myristic acid, the protocol we used offers a way to uniformly attach lauric acid, a naturally occurring post-translational modification, to a protein by using the single vector system pETDuet-1 for coexpression of the protein and human N-myristoyltransferase in *Escherichia coli* cells. To our knowledge, this method is a so far not described way to achieve this post-translational modification in a uniformly way.

8.2. Liposome and calcium binding of BASP1

Myristoylated proteins are often found in signal transduction pathways [44]. One example is recoverin, a myristoylated protein found in the retina that functions as a Ca^{2+} sensor. It belongs to the EF-hand family and can experience a calcium myristoyl switch; upon binding of calcium, the myristoyl group that was buried in a hydrophobic pocket of the protein is exposed and binds to membranes [45]. The calcium binding loop of recoverin resembles the calcium binding region of BASP1 found between residues 59-70. The same coordination loop is found in the four calcium-coordination sites of calmodulin. The binding loop of calmodulin is composed of twelve amino acids and coordinates calcium (see figure 15) by binding the ion through side chain interactions of residues on loop position 1,3,5,9 (*via* H_2O) and 12 and by backbone interaction of residue 7 [46].

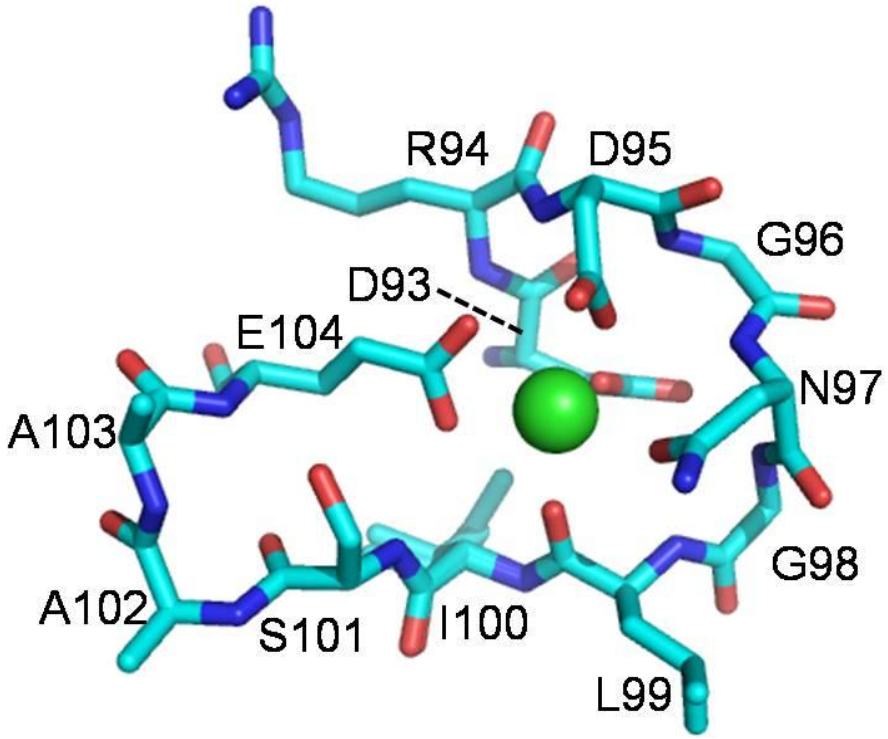

Figure 15: Calmodulin binding loop 3 (residues 93-104; PDB entry 1EXR). The binding of the calcium ion (green) is accomplished by side chain interactions of D93, D95, N97, S101 (via a water molecule) and E104 and main chain interaction of residue L99.

loop position	1	2	3	4	5	6	7	8	9	10	11	12
CaM loop1	D	K	D	G	D	G	T	I	T	T	K	E
CaM loop2	D	A	D	G	N	G	T	I	D	F	P	E
CaM loop3	D	R	D	G	N	G	L	I	S	A	A	E
CaM loop4	D	I	D	G	D	G	H	I	N	Y	E	E
BASP1	D	Q	D	A	E	G	K	A	E	E	K	E

Figure 16: Comparision of the sequence of the four EF-hand Ca^{2+} co-ordination loops of calmodulin and the calcium binding site of BASP1. The CaM sequence was taken from the PDB entry 1EXR. Loop1- residues 20-31; loop2 56-67; loop 393-104 and loop4 129-140. Residues 59-70 are shown for BASP1. Identical amino acids on the same loop position are labeled in blue.

The most conserved positions in the canonical EF-hand coordination loop are the aspartate on loop position 1, the glycine on position 6 and the glutamate on position 12 [46]. Those residues are important to form the bipyramidal co-ordination sphere and all of them are present in BASP1 at the canonical positions (see figure 16). The calcium binding loop of recoverin also has those three conserved residues at the expected positions. When measuring the paramagnetic effect of manganese on BASP1, the peak height of the residues in this binding loop between residues 59-70 is clearly decreased at a Mn^{2+}- concentration of 10µM where there is no significant effect on the rest of the protein. The chemical shift change upon calcium addition is strongest for that part, which indicates that there is a specific interaction at this site. In order to test the similarity of the binding mode of the coordination loop of calmodulin and the calcium-binding of BASP1, the distance-dependence of the paramagnetic effect of manganese is exploited according to Ubach *et al* [35]. The distance of the calcium ion to the backbone of the four coordination loops of calmodulin in the crystal structure is related to the decrease of the cross-peak intensities of the ^{1}H-^{15}N- HSQC spectrum of BASP1 upon manganese addition and should result in a negative slope (see figure 17). The result is an indication of the binding mode of calcium to the binding site of BASP1 between residues 59-70 which could be similar to the calcium binding site of calmodulin.

Chemical shifts data (see figure 4) indicate, that a transient helix-loop-helix motif could be present, but further characterization is necessary.

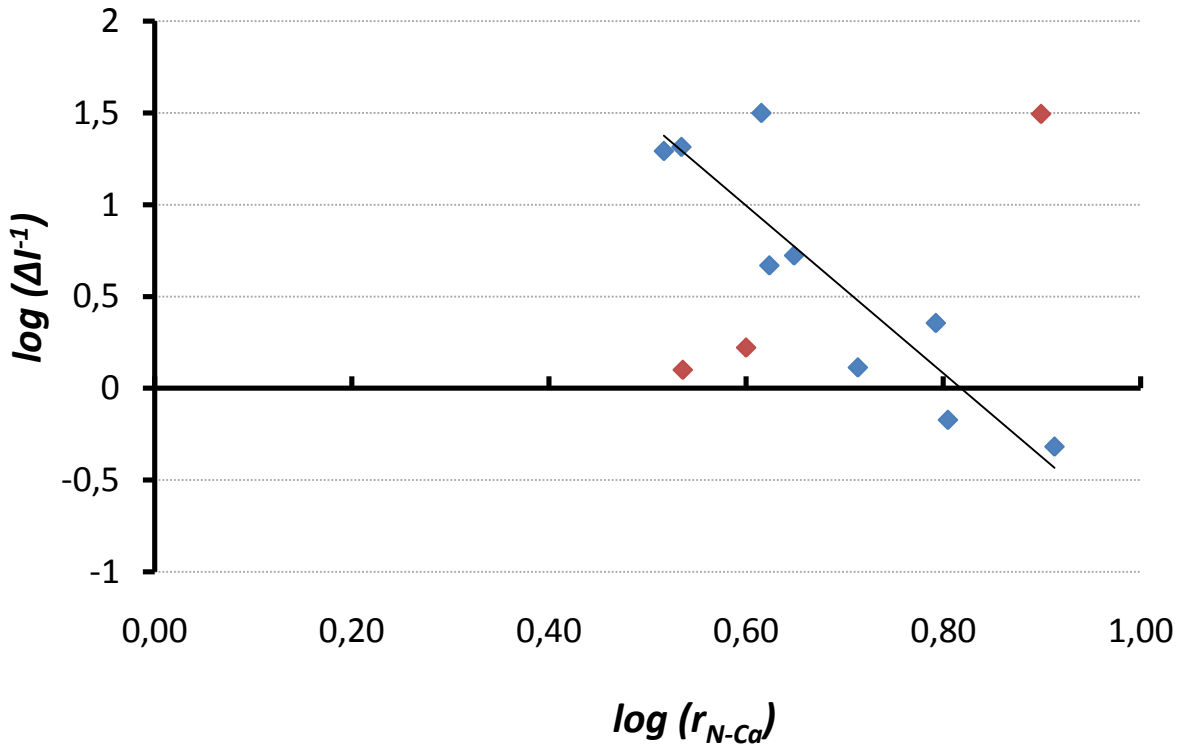

Figure 17: Correlation of the distance of the calcium ion of the co-oordination loop of calmodulin and the paramagnetic effect of manganese on BASP1. The distances were extracted from the PDB entry 1EXR. The coordination loop is composed of twelve residues. Δr^{-1} is the difference of the inverted normalized intensity of the cross peaks of the spectrum recorded with manganese and the inverted normalized intensity of the reference spectrum. $r_{N\text{-}Ca}$ is the average of distance of the calcium ion to the nitrogen backbone of the four binding loops of calmodulin. Not all cross peaks of the binding region are separated in the spectrum so the red dots are considered as outliers.

In contrast to recoverin, BASP1 is bound to the membrane in the absence of calcium and is released from the membrane when the calcium concentration increases. Since BASP1 is involved in the PIP2-signaling pathway, where calcium plays a major role, the calcium- dependent membrane detachment could be an important feature of the protein. Local concentration of calcium at specialized microdomains, lipid rafts, can be up to hundreds of µM [47, 48], so the presented results can be of relevance *in vivo*. Lipid rafts are known to contain proteins involved in Ca^{2+}-signaling pathways and Ca^{2+}-channels ; they are highly specialized microdomains to transduce calcium-dependent signals (reviewed in [49]) and both BASP1 as well as PIP2 are located in lipid rafts.

Liposome binding assay and NMR data indicate that there is an interaction of the N-terminal domain of unmyristoylated BASP1 with the Folch liposomes, probably due to an electrostatic interaction of the basic patch with lipid headgroups. *In vitro* binding ability of myristoylated BASP1 depends on the lipid composition of the liposomes used [50], with PIP2, phosphatidylethanolamine and cholesterol increasing binding of the protein.

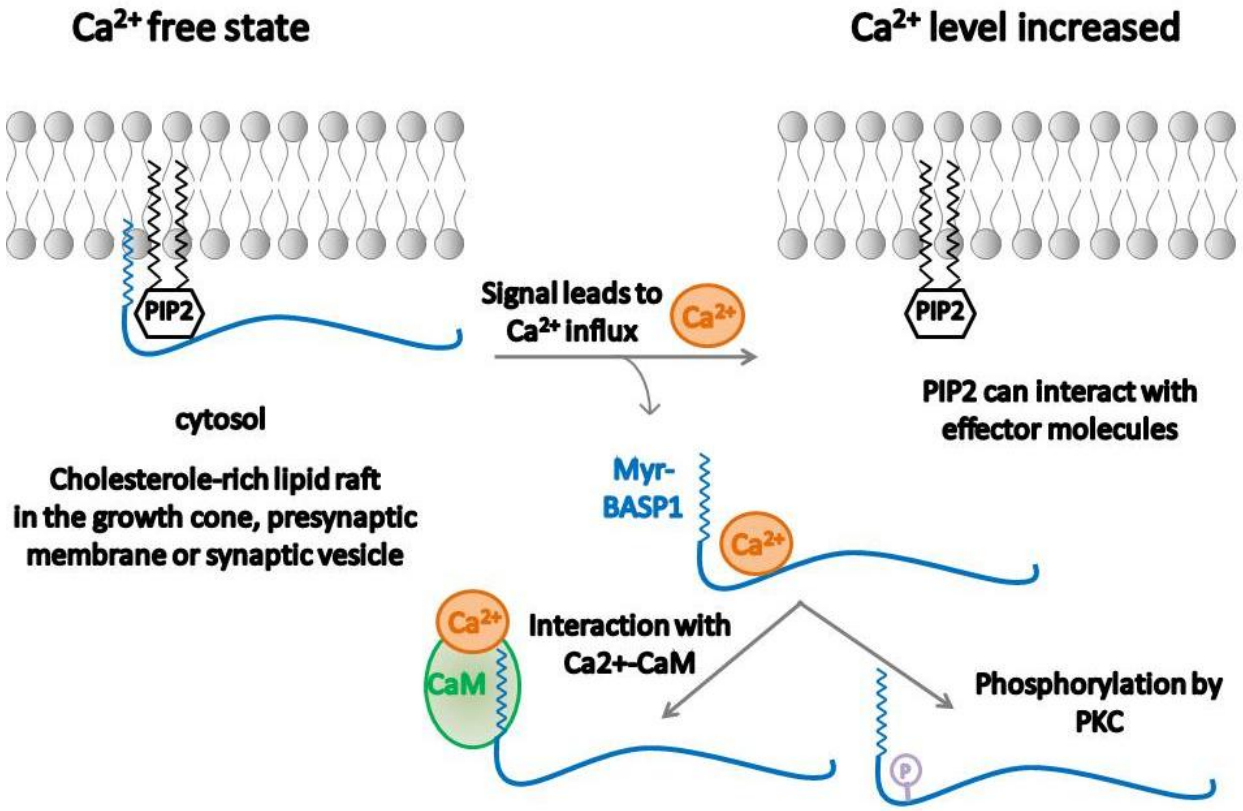

Figure 18: Proposed model of the interaction of BASP1 and PIP2 at lipid rafts.

The overall function of BASP1 beside the sequestration of PIP2 into specialized microdomains, lipid rafts, in a cholesterol-dependent manner, is a protective role for PIP2, preventing its modification by phosphatases and lipases [3, 17]. An incoming signal and a resulting calcium increase leads to membrane detachment of BASP1 while PIP2 stays at the membrane. This enables PIP2 to act as a second messenger, to be cleaved or modified for signaling. When BASP1 is not bound to the membrane

anymore, it can interact with Ca^{2+}-calmodulin or PKC. Once the calcium level is decreased again, BASP1 is released from calmodulin or is dephosphorylated by phosphatases and can bind to lipid rafts again. These interactions are summarized in figure 18.

Both growth cone guidance and neurotransmitter release are PIP2 and calcium-dependent processes. BASP1 is found in the growth cone, synaptic vesicles and the presynaptic membrane; the calcium dependent membrane detachment and the subsequent release of PIP2 from BASP1 in response to a signal which leads to a rise in the local calcium concentration, could be an important mechanism to control PIP2 cleavage and phosphorylation status. BASP1 can help to coordinate PIP2 activity and modification and restrict the release of PIP2 from BASP1 in a Ca^{2+}- dependent manner.

If detachment of BASP1 from the membrane is due to calcium binding to the protein, it is an interesting new feature of this intrinsically disordered protein and is a new example of how IDPs can act in the cell, especially in signaling pathways.

9. Conclusion

We described here some new features of BASP1 that can prove to be relevant for the proteins' function *in vivo.* BASP1 can bind to Ca^{2+} and seems to have a calcium coordination loop that resembles the coordination sphere found in calmodulin. Upon calcium addition, the protein detaches from liposomes *in vitro* and the detachment is not influenced by the binding partner calmodulin.

The presented results can be used as a basis for further characterization of BASP1s interaction with different partners. Of particular interest will be the binding mode to calcium and the release of the protein from the membrane. The first step would be the purification of a ^{15}N-labeled fully myristoylated sample for NMR- measurement. Once this step is done, the two forms of BASP1 (myristoylated and lauroylated) can be used to study the different properties of these modifications on liposomes or calmodulin binding and investigate on structural and dynamic features. Further experiments will include the binding properties of BASP1 to liposomes using different lipid compositions in order to identify the lipid composition that is influencing binding of both myristoylated and unmyristoylated BASP1. To accomplish this task, a GFP construct of BASP1 will be designed to be able to quantify binding to liposomes based on fluorescence measurement. The effect of phosphorylation on liposome binding is another interesting topic. It is not clear what influence this post-translational modification will have on the dynamics of BASP1. Further characterization of the detachment from liposomes can be done by studying mutants of the protein. Finally, the interaction mode of calmodulin with BASP1 will be of great interest.

10. References

1. Maekawa S, Maekawa M, Hattori S, Nakamura S. Purification and molecular cloning of a novel acidic calmodulin binding protein from rat brain. J Biol Chem 1993; 268: 13703-13709.

2. Laux T, Fukami K, Thelen M et al. GAP43, MARCKS, and CAP23 modulate PI(4,5)P(2) at plasmalemmal rafts, and regulate cell cortex actin dynamics through a common mechanism. J Cell Biol 2000; 149: 1455-1472.

3. Takaichi R, Odagaki S, Kumanogoh H et al. Inhibitory effect of NAP-22 on the phosphatase activity of synaptojanin-1. J Neurosci Res 2012; 90: 21-27.

4. Falkenburger BH, Jensen JB, Dickson EJ et al. Phosphoinositides: lipid regulators of membrane proteins. J Physiol 2010; 588: 3179-3185.

5. Moss SE. How actin gets the PIP. Sci Signal 2012; 5: pe7.

6. Koch M, Holt M. Coupling exo- and endocytosis: an essential role for PIP(2) at the synapse. Biochim Biophys Acta 2012; 1821: 1114-1132.

7. Saarikangas J, Zhao H, Lappalainen P. Regulation of the actin cytoskeleton-plasma membrane interplay by phosphoinositides. Physiol Rev 2010; 90: 259-289.

8. Kaksonen M, Toret CP, Drubin DG. Harnessing actin dynamics for clathrin-mediated endocytosis. Nat Rev Mol Cell Biol 2006; 7: 404-414.

9. Tojima T. Intracellular signaling and membrane trafficking control bidirectional growth cone guidance. Neurosci Res 2012; 73: 269-274.

10. Dent EW, Gupton SL, Gertler FB. The growth cone cytoskeleton in axon outgrowth and guidance. Cold Spring Harb Perspect Biol 2011; 3.

11. Yamamoto Y, Sokawa Y, Maekawa S. Biochemical evidence for the presence of NAP-22, a novel acidic calmodulin binding protein, in the synaptic vesicles of rat brain. Neurosci Lett 1997; 224: 127-130.

12. Iino S, Kobayashi S, Maekawa S. Immunohistochemical localization of a novel acidic calmodulin-binding protein, NAP-22, in the rat brain. Neuroscience 1999; 91: 1435-1444.

13. Kashihara M, Miyata S, Kumanogoh H et al. Changes in the localization of NAP-22, a calmodulin binding membrane protein, during the development of neuronal polarity. Neurosci Res 2000; 37: 315-325.

14. Li H, Papadopoulos V. Peripheral-type benzodiazepine receptor function in cholesterol transport. Identification of a putative cholesterol recognition/interaction amino acid sequence and consensus pattern. Endocrinology 1998; 139: 4991-4997.

15. Epand RM, Vuong P, Yip CM et al. Cholesterol-dependent partitioning of PtdIns(4,5)P2 into membrane domains by the N-terminal fragment of NAP-22 (neuronal axonal myristoylated membrane protein of 22 kDa). Biochem J 2004; 379: 527-532.

16. Epand RF, Sayer BG, Epand RM. Induction of raft-like domains by a myristoylated NAP-22 peptide and its Tyr mutant. FEBS J 2005; 272: 1792-1803.

17. Taguchi K, Kumanogoh H, Nakamura S, Maekawa S. Localization of phospholipase C beta 1 on the detergent-resistant membrane microdomain prepared from the synaptic plasma membrane fraction of rat brain. J Neurosci Res 2007; 85: 1364-1371.

18. Perera RM, Zoncu R, Lucast L et al. Two synaptojanin 1 isoforms are recruited to clathrin-coated pits at different stages. Proc Natl Acad Sci U S A 2006; 103: 19332-19337.

19. Matsubara M, Nakatsu T, Kato H, Taniguchi H. Crystal structure of a myristoylated CAP-23/NAP-22 N-terminal domain complexed with Ca2+/calmodulin. EMBO J 2004; 23: 712-718.

20. Maekawa S, Murofushi H, Nakamura S. Inhibitory effect of calmodulin on phosphorylation of NAP-22 with protein kinase C. J Biol Chem 1994; 269: 19462-19465.

21. Frey D, Laux T, Xu L et al. Shared and unique roles of CAP23 and GAP43 in actin regulation, neurite outgrowth, and anatomical plasticity. J Cell Biol 2000; 149: 1443-1454.

22. Korshunova I, Caroni P, Kolkova K et al. Characterization of BASP1-mediated neurite outgrowth. J Neurosci Res 2008; 86: 2201-2213.

23. Green LM, Wagner KJ, Campbell HA et al. Dynamic interaction between WT1 and BASP1 in transcriptional regulation during differentiation. Nucleic Acids Res 2009; 37: 431-440.

24. Carpenter B, Hill KJ, Charalambous M et al. BASP1 is a transcriptional cosuppressor for the Wilms' tumor suppressor protein WT1. Mol Cell Biol 2004; 24: 537-549.

25. Mosevitsky MI, Capony JP, Skladchikova G et al. The BASP1 family of myristoylated proteins abundant in axonal termini. Primary structure analysis and physico-chemical properties. Biochimie 1997; 79: 373-384.

26. Hartl M, Nist A, Khan MI et al. Inhibition of Myc-induced cell transformation by brain acid-soluble protein 1 (BASP1). Proc Natl Acad Sci U S A 2009; 106: 5604-5609.

27. Epand RM, Maekawa S, Yip CM, Epand RF. Protein-induced formation of cholesterol-rich domains. Biochemistry 2001; 40: 10514-10521.

28. Tompa P. Intrinsically disordered proteins: a 10-year recap. Trends Biochem Sci 2012; 37: 509-516.

29. Pancsa R, Tompa P. Structural disorder in eukaryotes. PLoS One 2012; 7: e34687.

30. Tamiola K, Acar B, Mulder FA. Sequence-specific random coil chemical shifts of intrinsically disordered proteins. J Am Chem Soc 2010; 132: 18000-18003.

31. Kragelj J, Ozenne V, Blackledge M, Jensen MR. Conformational Propensities of Intrinsically Disordered Proteins from NMR Chemical Shifts. Chemphyschem 2013.

32. Geist L, Zawadzka-Kazimierczuk A, Saxena S et al. (1)H, (13)C and (15)N resonance assignments of human BASP1. Biomol NMR Assign 2013; 7: 315-319.

33. Gluck JM, Hoffmann S, Koenig BW, Willbold D. Single vector system for efficient N-myristoylation of recombinant proteins in E. coli. PLoS One 2010; 5: e10081.

34. Schanda P, Brutscher B. Very fast two-dimensional NMR spectroscopy for real-time investigation of dynamic events in proteins on the time scale of seconds. J Am Chem Soc 2005; 127: 8014-8015.

35. Ubach J, Zhang X, Shao X et al. Ca2+ binding to synaptotagmin: how many Ca2+ ions bind to the tip of a C2-domain? EMBO J 1998; 17: 3921-3930.

36. Devaux PF. Static and dynamic lipid asymmetry in cell membranes. Biochemistry 1991; 30: 1163-1173.

37. Takamori S, Holt M, Stenius K et al. Molecular anatomy of a trafficking organelle. Cell 2006; 127: 831-846.

38. Kishore NS, Wood DC, Mehta PP et al. Comparison of the acyl chain specificities of human myristoyl-CoA synthetase and human myristoyl-CoA:protein N-myristoyltransferase. J Biol Chem 1993; 268: 4889-4902.

39. Bereta G, Palczewski K. Heterogeneous N-terminal acylation of retinal proteins results from the retina's unusual lipid metabolism. Biochemistry 2011; 50: 3764-3776.

40. Kokame K, Fukada Y, Yoshizawa T et al. Lipid modification at the N terminus of photoreceptor G-protein alpha-subunit. Nature 1992; 359: 749-752.

41. Neubert TA, Johnson RS, Hurley JB, Walsh KA. The rod transducin alpha subunit amino terminus is heterogeneously fatty acylated. J Biol Chem 1992; 267: 18274-18277.

42. Jung J, Byeon IJ, Ahn J, Gronenborn AM. Structure, dynamics, and Hck interaction of full-length HIV-1 Nef. Proteins 2011; 79: 1609-1622.

43. Tapp H, Al-Naggar IM, Yarmola EG et al. MARCKS is a natively unfolded protein with an inaccessible actin-binding site: evidence for long-range intramolecular interactions. J Biol Chem 2005; 280: 9946-9956.

44. Farazi TA, Waksman G, Gordon JI. The biology and enzymology of protein N-myristoylation. J Biol Chem 2001; 276: 39501-39504.

45. Zozulya S, Stryer L. Calcium-myristoyl protein switch. Proc Natl Acad Sci U S A 1992; 89: 11569-11573.

46. Gifford JL, Walsh MP, Vogel HJ. Structures and metal-ion-binding properties of the Ca2+-binding helix-loop-helix EF-hand motifs. Biochem J 2007; 405: 199-221.

47. Llinas R, Sugimori M, Silver RB. Microdomains of high calcium concentration in a presynaptic terminal. Science 1992; 256: 677-679.

48. Aharon S, Bercovier M, Parnas H. Parallel computation enables precise description of Ca2+ distribution in nerve terminals. Bull Math Biol 1996; 58: 1075-1097.

49. Pani B, Singh BB. Lipid rafts/caveolae as microdomains of calcium signaling. Cell Calcium 2009; 45: 625-633.

50. Terashita A, Funatsu N, Umeda M et al. Lipid binding activity of a neuron-specific protein NAP-22 studied in vivo and in vitro. J Neurosci Res 2002; 70: 172-179.

11. Acknowledgements

I would like to thank my family and friends, especially my parents for their encouragement for my studies.

Also I would like to acknowledge the cooperation with Kathrin Breuker from the University of Innsbruck for doing the mass spectrometry and Sasha Martens and Marta Walczak for their help in preparing the liposomes.

Special thanks to Robert Konrat for enabling this master thesis in his lab and for guiding me during this year and Nicolas Coudevylle for his fruitful support as a supervisor as well as all people from this lab for creating a familiar and constructive atmosphere at work.

12. Appendices

12.1. Zusammenfassung

BASP1 (human brain acid soluble protein 1) ist ein N-terminal myristoyliertes, intrinsisch ungeordnetes Protein, welches im neuronalen Phosphatidylinositol 4,5-bisphosphate (PIP2) Signaltransduktionsweg involviert ist. Welche Rolle BASP1 in diesem Prozess spielt ist noch nicht geklärt, jedoch scheint dieses Protein an der neuronalen Wachstumskegelformation und Neurotransmitterausschüttung beteiligt zu sein. BASP1 bindet an cytosolischer Seite der Plasmamembran. Eine wichtige Funktion von BASP1 ist die Cholesterol-abhängige Sequesterierung von PIP2 in Lipid rafts der präsynaptischen Membran oder des axonalen Wachtumskegels.

Ziel dieser Arbeit ist es, mittels Kernspinresonanz (NMR) und anderen biophysikalischen Methoden, den Einfluss der N-Myristoylierung auf die strukturellen Dynamiken von BASP1, besonders auf die Konsequenzen dieser Modifikation auf Interaktionseingenschaften, zu untersuchen. Für diese Experimente muss BASP1 mit und ohne N-Myristoylierung rekombinant exprimiert werden. Es ist uns gelungen, rekombinant myristoyliertes BASP1 zu erhalten, indem wir humane N-myristoyltransferase und BASP1 in *Escherichia coli* Zellen co-exprimiert haben mittels einem dualen Expressionsvektors. Zusätzlich haben wir durch Massenspektrometrie zeigen können, dass rekombinante Expression von N-myristoyliertem BASP1 in minimal Medium, welchen für Isotopenlabeling benötigt wird, zu einer Mischung aus myristolierter und lauroylierter Form des Proteins führt.

Die strukturelle Dynamik der nativen und N-myristoylierten Form ist Thema dieser Arbeit; interessanterweise konnten wir zeigen, dass beide Formen Ca^{2+} direkt binden können und Calcium zu einem Lösen von BASP1 von Liposomen in vitro führt. Dieses bisher unbekannte Feature von BASP1 könnte sich als relevant in vivo herausstellen, da BASP1 in Calcium abhängigen Prozessen wie dem PIP2 Signaltransduktionsweg, Neurotransmitterausschüttung oder Wachtumskegellenkung vorkommt.

12.2. Abbreviations

APS	ammonium persulfate
BASP1	Brain acid soluble protein 1
BCA	bicinchoninic acid
BSA	bovine serum albumin
CaM	calmodulin
CD	circular dichroism
CAP-23	cortical cytoskeleton-associated protein
CRAC	cholesterol recognition/interaction amino acid consensus pattern
DAG	diacylglycerole
E.coli	*Escherichia coli*
EDTA	ethylenediaminetetraacetic acid
ER	endoplasmatic reticulum
ESI-FT-ICR	electrospray ionization fourier transform ion cyclotron resonance
GFP	green fluorescent protein
HMQC	heteronuclear multiple quantum correlation
HSQC	heteronuclear single quantum correlation
IDP	intrinsically disordered protein
IP3	inositol 1,4,5-trisphosphate
IPTG	Isopropyl β-D-1-thiogalactopyranoside
NAP-22	neuron-specific acidic protein

NMR	nuclear magnetic resonance
NMT	N-myristoyltransferase
PAA	polyacrylamide
PI	phosphatidylinositol
PIP2	Phosphatidylinositol 4,5-bisphosphate
PIP3	phosphatidylinositol (3,4,5)-trisphosphate
PKC	Protein kinase C
RP-HPLC	Reverse phase high-pressure liquid chromatography
SDS-PAGE	sodium dodecyl sulfate polyacrylamide gel electrophoresis
SUMO-3	Small ubiquitin-related modifier 3
TEMED	Tetramethylethylenediamine
WT1	Wilms tumor protein

12.3. Lebenslauf

Name:	Andrea Gabriele Flamm, BSc
Schullaufbahn:	1995 - 1999 Volksschule Phorusgasse, 1040 Wien
	1999 - 2004 Wiedner Gymnasium, 1040 Wien
	2004 - 2007 Sir Karl Popper Schule, 1040 Wien
Universitäre Ausbildung:	2007 - 2008 FH Steyr –Internationales Logistik Management
	2008-2011: Universität Wien- Bachelorstudium Molekularbiologie
	2011-2013: Universität Wien- Masterstudium Molekularbiologie mit Spezialisierung auf molekulare Strukturbiologie mit dem Schwerpunkt nuclear magnetic resonance (NMR)